Resonant micro-Raman study of $Nd_{0.5}Sr_{0.5}MnO_3$

2005 J. Phys.: Condens. Matter 17 5247

(http://iopscience.iop.org/0953-8984/17/34/009)

INSTITUTE OF PHYSICS PUBLISHING JOURNAL OF PHYSICS: CONDENSED MATTER

J. Phys.: Condens. Matter **17** (2005) 5247–5254 doi:10.1088/0953-8984/17/34/009

Resonant micro-Raman study of $Nd_{0.5}Sr_{0.5}MnO_3$

S Asselin[1], S Jandl[1,4], P Fournier[1], A A Mukhin[2], V Yu Ivanov[2] and A M Balbashov[3]

[1] Département de Physique, Université de Sherbrooke, Sherbrooke, QC, J1K2R1, Canada
[2] General Physics Institute of the Russian Academy of Sciences, 38 Vavilov Street, 119991 Moscow, Russia
[3] Moscow Power Engineering Institute, 14 Krasnokazarmennaya Street, 105835 Moscow, Russia

Received 27 April 2005, in final form 6 July 2005
Published 12 August 2005
Online at stacks.iop.org/JPhysCM/17/5247

Abstract

We present a resonant micro-Raman study of a high-quality $Nd_{0.5}Sr_{0.5}MnO_3$ single crystal as a function of temperature. The detected phonons trace the evolution between the paramagnetic, ferromagnetic, A-type antiferromagnetic and CE-type antiferromagnetic charge and orbital ordering phase transitions. The 16 detected phonon frequencies at $T < T_{co}$ are compared to $NdMnO_3$ and $La_{0.5}Ca_{0.5}MnO_3$ observed frequencies, indicating the presence of coherent Jahn–Teller distortions and strong similarities between the CE-type $Nd_{0.5}Sr_{0.5}MnO_3$ and $La_{0.5}Ca_{0.5}MnO_3$ phases.

1. Introduction

Substitution of rare earth ions R^{3+} by divalent cations A^{2+} generates Mn^{4+} ions in $R_{1-x}A_xMnO_3$ (R = lanthanides and A = Ba, Sr, or Ca). While $RMnO_3$ compounds are antiferromagnetic with important Jahn–Teller distortions, lanthanide substitution leads to double-exchange interactions, reduction of Jahn–Teller-type distortions, charge and orbital ordering, and simultaneous observation of metallic and ferromagnetic characters for $x \sim 0.3$ [1–3]. Near either the concomitant paramagnetic insulator to ferromagnetic metallic phase transition [4], or ferromagnetic metallic to charge ordered insulator transition [5], a colossal negative magnetoresistance, reflecting strong interconnections between the electrical and magnetic properties, has been observed. The Mn^{3+}/Mn^{4+} distribution modifies the Mn–O bond lengths and provokes structural disorder that is strongly temperature and doping dependent. Charge ordering below T_{co}, which is favoured for the $x = 0.5$ composition, as a result of equal proportions of Mn^{3+} and Mn^{4+} ions, is also observed in the $0.3 < x < 0.75$ range depending on the R^{3+} and A^{2+} ions. Along with charge ordering, orbital ordering develops and CE-type insulating antiferromagnetic behaviour competes with the double-exchange interaction [6]. Whether doping, at different levels, results in homogeneous or coexisting phases remains an

[4] Author to whom any correspondence should be addressed.

important issue for theoretical modelling centred on phase separation [7]. In particular, it was found that electron-rich ferromagnetic and electron-poor antiferromagnetic domains can occur in charge ordered phases [8].

Compared to the La compounds, the Nd-based compounds have been less studied; they are nevertheless interesting since the strength of the double-exchange interactions is weaker due to larger lattice distortions provoked by the smaller Nd ions [9]. Consequently, in doped systems like $Nd_{1-x}(Ca, Sr)_xMnO_3$ as compared to $La_{1-x}(Ca, Sr)_xMnO_3$ closer competitions with new generic instabilities would exist between the electron–phonon, electron–electron and exchange interactions [10].

Phase separation may be expected in $Nd_{0.5}Sr_{0.5}MnO_3$, which is at the phase boundary separating the charge disordered A-type antiferromagnetic phase from the CE-type charge ordered phase [11]. Also the onset of its charge ordering, around $T_{co} \sim 150$ K, is accompanied by marked jumps in resistivity and magnetization [12].

At $T = 300$ K, $Nd_{0.5}Sr_{0.5}MnO_3$ is paramagnetic and its structure is orthorhombic ($Imma$). With lowering temperature, it first becomes ferromagnetic (∼250 K) and then a phase fraction of A-type antiferromagnetism characterized by $d_{(z^2-x^2)}$ orbital ordering appears around 220 K without changing the $Imma$ symmetry. In this new phase, the $a(x)$ and $c(y)$ parameters increase while the $b(z)$ parameter decreases [13]. Around 150 K a charge-ordered phase, characterized by CE-type antiferromagnetism with $d_{(3x^2-r^2)}$ and $d_{(3z^2-r^2)}$ orbital ordering on the Mn^{3+} sites, develops in a monoclinic ($P2_1/m$)-type structure. The ferromagnetic charge and orbital ordered zigzag chains formed in the xz plane are coupled antiferromagnetically to each other along the y axis [14, 15]. Under 6 T magnetic field, the charge-ordered monoclinic phase transforms into the metallic ferromagnetic phase [14]. It is important to note that $Nd_{1-x}Sr_xMnO_3$ is stable in the very narrow doping range $0.48 < x < 0.51$ [15], rendering $Nd_{0.5}Sr_{0.5}MnO_3$ single-crystal growth very stringent.

Raman spectroscopy has proved its efficiency in the characterization of the mixed valence manganite disorder with the detection of the oxygen partial phonon density of states and phase separation [7, 16]. Abrashev *et al* [17] have studied by Raman spectroscopy the charge and orbital ordered state in $La_{0.5}Ca_{0.5}MnO_3$. They observed that the new activated Raman modes, below $T \sim 150$ K, in the antiferromagnetic insulating ordered state were enhanced when excited with laser energies close to the Jahn–Teller gap, ∼1.9 eV [18]. The most intense modes were assigned in comparison with layered manganites and undoped $RMnO_3$ (R = La, Y).

Kuroe *et al* [19] and Choi *et al* [20] have studied $Nd_{0.5}Sr_{0.5}MnO_3$ Raman active modes as a function of temperature, limiting their analysis to the low temperature state. Both groups used a macro-Raman set-up and the 514.5 nm Ar^+ ion laser line (2.4 eV) and did not resolve as many excitations as detected in $La_{0.5}Ca_{0.5}MnO_3$. Recently, Seikh *et al* [21] observed in $Nd_{0.5}Sr_{0.5}MnO_3$ broad Raman active bands superimposed on electronic background at $T > 150$ K. The linewidths of all the fitted modes even at low temperature, down to 50 K, were very large.

In this paper we present a study of $Nd_{0.5}Sr_{0.5}MnO_3$ Raman active modes under a microscope pinpointing on ∼3 μm diameter areas. We have selected twinning free high quality single micro-crystals in order to verify the phonon associated selection rules and we have used the 632.8 nm (1.96 eV) He–Ne laser line so that the phonon intensities became resonantly enhanced as predicted around 1.9 eV [18]. Our objectives are (i) to determine if the Raman active excitations reflect the evolution of the multiple phase transitions between room temperature and 20 K, (ii) to compare the two systems $Nd_{0.5}Sr_{0.5}MnO_3$ and $La_{0.5}Ca_{0.5}MnO_3$, and (iii) to detect if phase separation develops at various temperatures as inferred by recent models [7].

2. Experiments

The $Nd_{0.5}Sr_{0.5}MnO_3$ single crystal, typically platelike with (001) oriented faces (∼1 mm, 2 mm, 200 μm), was grown by the floating zone method as described in [22]. 0.5 cm^{-1} resolution Raman spectra were measured in the backscattering configuration using a He–Ne laser (632.8 nm) and a Labram-800 Raman microscope spectrometer equipped with × 50 objective, appropriate notch filter and nitrogen cooled CCD detector. The sample was mounted on the cold finger of a micro-helium Janis cryostat with the z-axis ($Imma$ symmetry) parallel to the incident radiation and the laser power was kept at 0.8 mW to avoid local heating. A_g and B_{2g} symmetry phonons were detected, similarly to the study of $La_{0.5}Ca_{0.5}MnO_3$ [17], in the following configurations as indicated by the incident and scattered polarization directions: xx(A_g and B_{2g}), $x'x'$(A_g), and $x'y'$ (B_{2g}); x, x', and y' being along the [100], [110] and [$\bar{1}$10] quasicubic directions respectively. Twinnings occur unavoidably in platelike $Nd_{0.5}Sr_{0.5}MnO_3$. In order to establish unambiguous Raman scattering selection rules, untwined microcrystals within the sample need to be identified by using the Raman microscope. Such microcrystals are located when the A_g Raman active phonons obtained in the ($x'x'$) configuration become absent in the ($x'y'$) configuration in which only the B_{2g} symmetries are allowed. The sample is rotated till the incident laser beam polarization aligns with the x' axis so that pure A_g or B_{2g} symmetries are observed depending on the analyser orientation. With the incident polarization fixed, rotating further the sample by 45° permits the setting of the xx and xy configurations.

Absence of spurious signals was verified by the reproducibility of various microcrystal spectra and their corresponding selection rules.

The electrical resistivity was measured by the four-point direct current method in the 4–300 K temperature range. The magnetization was measured by means of a vibration sample magnetometer in magnetic fields up to 14 kOe and the AC magnetic susceptibility was obtained by a mutual inductance method at temperatures varying from 4 to 300 K.

3. Results and discussion

For our study, we have cut a specimen from a single crystal whose resistivity, magnetization and AC susceptibility were previously measured to insure the sample quality and occurrence of the expected $Nd_{0.5}Sr_{0.5}MnO_3$ phase transitions. In figure 1, the various electrical and magnetic properties of the sample retrace its temperature evolution and attest to its high quality as evidenced by the sharpness of the phase transitions. Particularly noticeable is the insulating charge ordered state manifestation around $T_N = 150$ K, which is known to be a first order transition.

In figure 2(a), $Nd_{0.5}Sr_{0.5}MnO_3$ Raman spectra at temperatures between 280 and 130 K are presented. At 280 K, we observe three bands centred at ∼205, 415 and 444 cm^{-1}. As the temperature is lowered, an additional wide band emerges from the background around 335 cm^{-1}. In the same temperature range, three broad bands were detected in $La_{0.5}Ca_{0.5}MnO_3$ ∼ 230, 450 and 610 cm^{-1} [17]. They were associated with the insulating high-temperature phase of the manganite rotation-like mode (∼230 cm^{-1}) which measures the rotational [23] and the Jahn–Teller (∼450 and 610 cm^{-1}) distortions respectively. In $Nd_{0.5}Sr_{0.5}MnO_3$, while only a broad band around 200 cm^{-1} was detected by Kuroe *et al* [19] in the 300–150 K temperature range, Choi *et al* [20] observed two bands around 200 and 450 cm^{-1} and Seikh *et al* [21] reported two additional broad bands around 340 and 600 cm^{-1}. In contrast to these previous measurements, the relative intensities of our three room temperature bands are evolving between 200 and 180 K, underlying the gradual arising of the A-type antiferromagnetic phase. The net increase of the 444 cm^{-1} phonon intensity

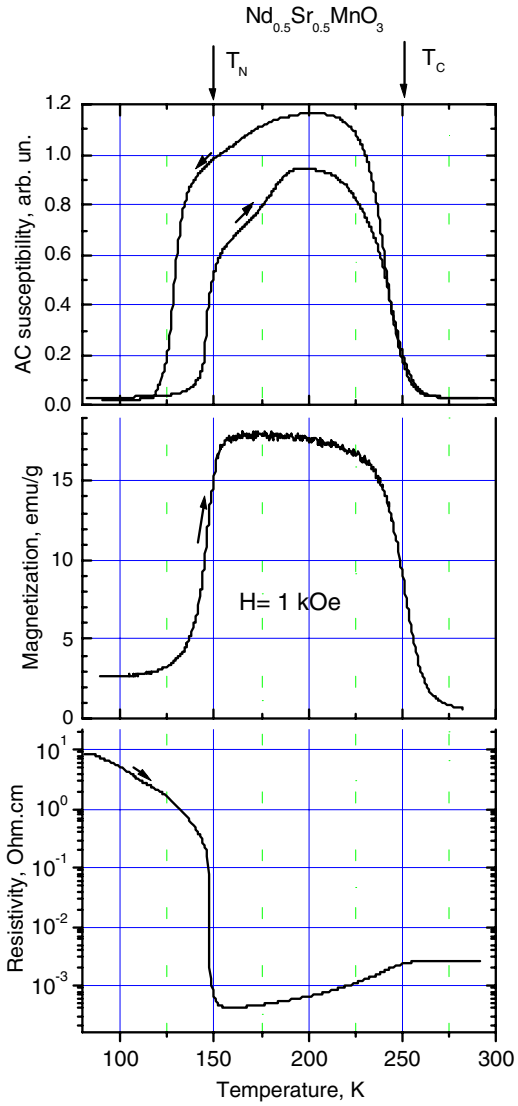

Figure 1. $Nd_{0.5}Sr_{0.5}MnO_3$ single-crystal AC susceptibility, magnetization and resistivity as a function of temperature.

(This figure is in colour only in the electronic version)

and the appearance of a broad band around 335 cm^{-1} characterize the ferromagnetic-A type antiferromagnetic phase changes. No disorder induced broad band, around 600 cm^{-1}, has been observed, attesting to the sharp stoichiometry and overall sample quality.

Below $T = 130$ K, with the occurrence of the CE-type antiferromagnetism (monoclinic ($P2_1/m$)-type structure), many Raman active phonons are observed (figure 2(b)) and compared to previous observations in $NdMnO_3$, $Nd_{0.5}Sr_{0.5}MnO_3$ and $La_{0.5}Ca_{0.5}MnO_3$ (table 1).

The monoclinic low symmetry and the consequent large number of Raman allowed modes (54) hinder the vibration analyses. Nevertheless, similarly to $La_{0.5}Ca_{0.5}MnO_3$ [17], $Nd_{0.5}Sr_{0.5}MnO_3$ may be associated with a simplified *pmma* structure that allows an association

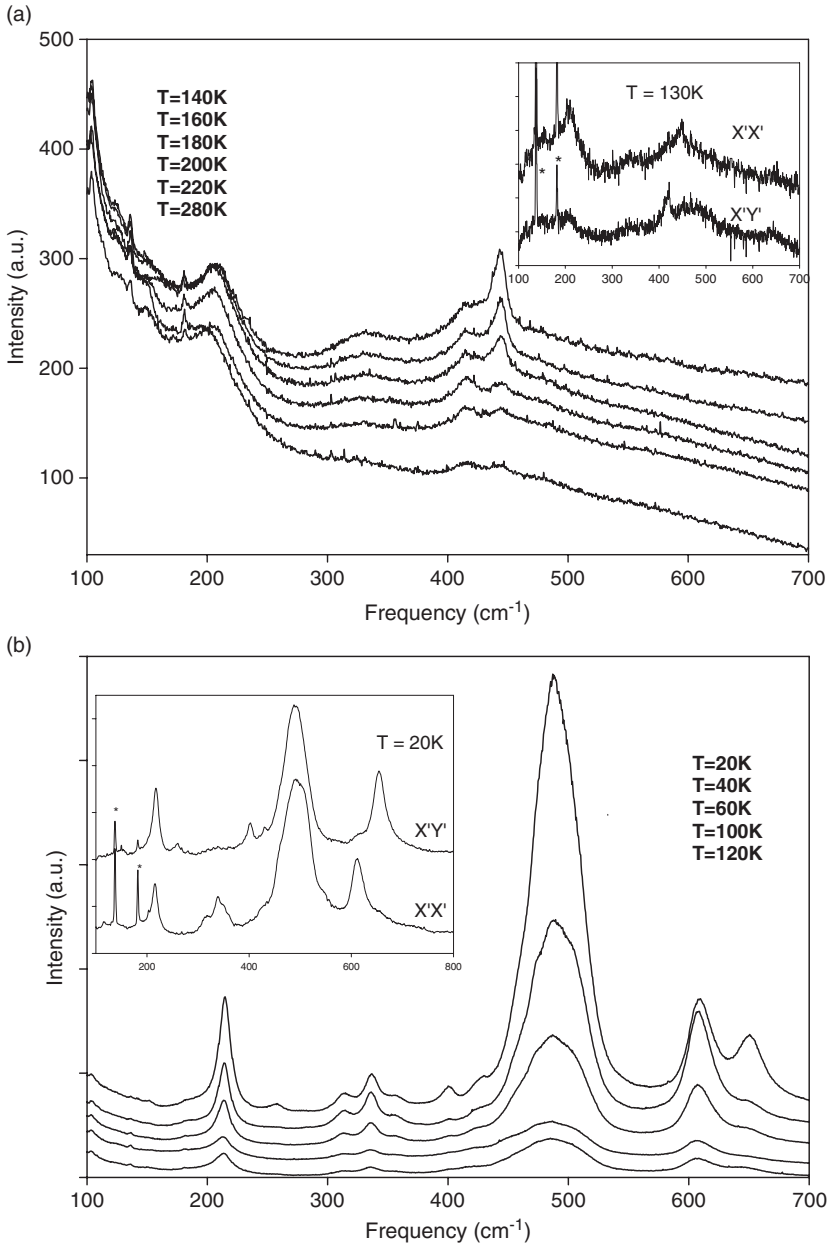

Figure 2. (a) $Nd_{0.5}Sr_{0.5}MnO_3$ single-crystal Raman active phonons, in the xx scattering configuration, as a function of temperature (top to bottom). * indicates plasma lines. Inset: 130 K Raman spectra in the $x'x'$ and $x'y'$ configurations. (b) $Nd_{0.5}Sr_{0.5}MnO_3$ single-crystal Raman active phonons in the xx scattering configuration, as a function of temperature (top to bottom). * indicates plasma lines. Inset: 20 K Raman spectra in the $x'x'$ and $x'y'$ configurations.

with internal (stretching and bending) and external (translation and libration) modes. They may also be compared to the A_g and B_{2g} $NdMnO_3$ (*pnma* structure) Raman active phonons [24]. The four strongest $NdMnO_3$ Raman active modes, 335 cm^{-1} (out of phase octahedral tilting),

Table 1. Raman frequencies, in cm^{-1}, of $La_{0.5}Ca_{0.5}MnO_3$, $NdMnO_3$ and $Nd_{0.5}Sr_{0.5}MnO_3$ for $T < T_{CO} \approx 150$ K. * indicates vibrations associated with orthorhombic $Nd_{0.5}Sr_{0.5}MnO_3$ for $T > T_{CO} \approx 150$ K and (s) refers to strong intensities.

$La_{0.5}Ca_{0.5}MnO_3$ [17]	$NdMnO_3$ [24]	$Nd_{0.5}Sr_{0.5}MnO_3$ [19]	$Nd_{0.5}Sr_{0.5}MnO_3$ [20]	$Nd_{0.5}Sr_{0.5}MnO_3$ [21]	$Nd_{0.5}Sr_{0.5}MnO_3$ This work
A_g	A_g	A_g			A_g
		79	74		82
	205	212	216	∼215	
233	245				214*(s)
319					316*
337(s)	335(s)	333	334	∼350	337*(s)
359					358*
	468				458*
487(s)	495(s)	484	490	490	489(s)
516(s)					509(s)
					543
601(s)		606	612	∼620	610(s)
B_{2g}	B_{2g}	B_{2g}			B_{2g}
		66			
217(s)		212			216*(s)
270		256			258
	314				
401		400	402		401
429					428*
	453		455	∼460	
473	482	481			475(s)
	500				
	601(s)				
643		650	664	660	651(s)

482 cm^{-1} (octahedral basal oxygens out of phase stretching), 495 cm^{-1} (octahedral basal oxygens out of phase bending) and 601 cm^{-1} (octahedral basal oxygens in phase stretching) phonons are observed in $Nd_{0.5}Sr_{0.5}MnO_3$ at 337, 475, 489 and 610 cm^{-1} respectively and have their corresponding phonons in $La_{0.5}Ca_{0.5}MnO_3$ at 337, 473, 487 and 601 cm^{-1} [17]. In contrast to the 601 cm^{-1} $NdMnO_3$ phonon, which softens as temperature is lowered below the A-type antiferromagnetic transition (∼75 K), the 610 cm^{-1} phonon is not affected by the CE-type antiferromagnetism. It manifests a frequency increase at low temperatures, 607 cm^{-1} at 100 K as compared to 610 cm^{-1} at 4.2 K. This overall behaviour underlines the sensitivity of the spin-phonon coupling, caused by the phonon modulation of the nearest neighbour exchange integral [25], to the spin ordering in the xz plane. Actually, in the xz planes, that stack antiferromagnetically along the y axis, the spin ordering is ferromagnetic in the A-type whereas it is somewhat complex in the CE-type [6]. The $NdMnO_3$ 645 cm^{-1} density of states infrared and Raman active excitation, which plays an important role in the multiphonon processes and orbital coupling [26], and the 453 cm^{-1} phonon, are also present in $Nd_{0.5}Sr_{0.5}MnO_3$ at 651 and 458 cm^{-1} respectively. Remarkably, the 651 cm^{-1} excitation hardening, almost 10 cm^{-1} between 100 and 4.2 K, possibly reflects an increase of the phonon–orbital interaction with the orbital ordering. In addition to the $NdMnO_3$ phonons, the 319, 359, 516, 217, 270, 401 and 429 cm^{-1} $La_{0.5}Ca_{0.5}MnO_3$ phonons, whose vibrational pattern has been described in [17], have their corresponding phonons in $Nd_{0.5}Sr_{0.5}MnO_3$ at 316, 358, 509, 216, 258, 401 and 428 cm^{-1}.

The strong similarities between the $Nd_{0.5}Sr_{0.5}MnO_3$ and $La_{0.5}Ca_{0.5}MnO_3$ Raman active phonons are indicative of the universal character of charge and orbital ordering in the manganites. Between 280 and 140 K, in the ferromagnetic and A-type antiferromagnetic phases, the 335, 415 and 444 cm^{-1} bands are possibly induced by dynamical non-spatially coherent Jahn–Teller distortions [27]. The 205 cm^{-1} broad band could be associated with the soft mode observed in rhombohedral $LaMnO_3$ [23] and $La_{1-x}Sr_xMnO_3$ [28], reflecting the presence of rhombohedral distortions. These excitations are observed below 140 K; the broad band around 335 cm^{-1} is resolved into three bands, 316, 337 and 358 cm^{-1}, the 415 and 444 cm^{-1} bands are blueshifted to 428 and 458 cm^{-1} and the 205 cm^{-1} band resolves into two bands, 214 and 216 cm^{-1}.

Persistence of the high temperature phase phonons below 140 K is indicative of phase separation occurrence at low temperatures in $Nd_{0.5}Sr_{0.5}MnO_3$. Also below 140 K, appearance of the 489 and 610 cm^{-1} strong phonon excitations implies that static and coherent Jahn–Teller distortions [27] are compatible with charge and orbital ordering as observed in the layered manganites [29]. Finally, we associate the 82, 258, 401, 509 and 543 cm^{-1} phonons, which are observed only at low temperatures in $Nd_{0.5}Sr_{0.5}MnO_3$ and are absent in $NdMnO_3$, with orbital and charge ordering.

4. Conclusion

$Nd_{0.5}Sr_{0.5}MnO_3$ resonant Raman scattering has allowed the observation of four and 16 Raman active modes above and below $T = T_{co}$ respectively. The observed phonons, as a function of temperature, trace the evolution of the A-type antiferromagnetic and CE-type antiferromagnetic phase transitions. Persistence of the high temperature phonons in the low temperature phase evidences the occurrence of phase separation in the material. Below T_{co}, $Nd_{0.5}Sr_{0.5}MnO_3$ and $La_{0.5}Ca_{0.5}MnO_3$ low temperature phonon frequencies are very similar. This indicates that, in addition to the identical crystalline structures, the charge and orbital ordering are also similar. Interestingly, the phonon comparison with $NdMnO_3$ reflects a coherent ordering of the Jahn–Teller distortions in the CE-antiferromagnetic phase as inferred previously for $La_{0.5}Ca_{0.5}MnO_3$ and layered manganites.

Acknowledgments

S Asselin, S Jandl and P Fournier acknowledge support from the National Science and Engineering Research Council of Canada, the Canadian Institute for Advanced Research and the Fonds Québécois de la Recherche sur la Nature et les Technologies. This work was supported in part by the Russian Foundation for Basic Research (03-02-16759) and the Quantum Macrophysics Program of the Russian Academy of Sciences.

References

[1] Zener C 1951 *Phys. Rev.* **82** 403
[2] Jim S, Tiefel T H, McCormack M, Fastnacht R, Ramesh R and Chen L H 1994 *Science* **264** 413
[3] Khomskii D I and Sawatzky G A 1997 *Solid State Commun.* **102** 87
[4] Coey J M D, Viret M and von Molnar S 1999 *Adv. Phys.* **48** 167
[5] Uehara M, Mori S, Chen C H and Cheong S W 1999 *Nature* **399** 560
[6] Rao C N R, Arulraj A, Cheetham A K and Raveau B 2000 *J. Phys.: Condens. Matter* **12** R83
[7] Dagotto E, Burgy J and Moreo A 2003 *Solid State Commun.* **126** 9
[8] Salamon M B and Jaime M 2001 *Rev. Mod. Phys.* **73** 583

[9] Caignaert V, Millange F, Hervieu M, Suard E and Raveau B 1996 *Solid State Commun.* **99** 173
[10] Tokunaga M, Miura N, Tomioka Y and Tokura Y 1998 *Phys. Rev.* B **57** 5259
[11] Ramirez A P 1997 *J. Phys.: Condens. Matter* **9** 8171
[12] Popov Y F, Kadomtseva A M, Vorob'ev G P, Kamilov K I, Shotfich Y S, Ivanov V Y, Mukhin A A and Balbashov A M 2003 *Phys.—Solid State* **45** 1280
[13] Woodward P M, Cox D E, Vogt T, Rao C N R and Cheetham A K 1999 *Chem. Mater.* **11** 3528
[14] Ritter C, Mahendiran R, Ibarra M R, Morellon L, Maignan A, Raveau B and Rao C N R 2000 *Phys. Rev.* B **61** R9229
[15] Kajimoto R, Yoshizawa H, Kawano H, Kuwahara H, Tokura Y, Ohoyama K and Ohashi M 1999 *Phys. Rev.* B **60** 9506
[16] Iliev M N, Abrashev M V, Popov V N and Hadjiev V G 2003 *Phys. Rev.* B **67** 212301
[17] Abrashev M V, Bäckström J, Börjesson L, Pissas M, Kolev N and Iliev M N 2001 *Phys. Rev.* B **64** 144429
[18] Allen P B and Perebeinos V 1999 *Phys. Rev. Lett.* **83** 4828
[19] Kuroe H, Habu I, Kuwahara H and Sekine T 2002 *Physica* B **316/317** 575
[20] Choi K Y, Lemmens P, Güntherodt G, Pattabiraman M, Rangarajan G, Gnezdilov V P, Balakrishnan G, McK Paul D and Lees M R 2003 *J. Phys.: Condens. Matter* **15** 3333
[21] Seikh M M, Sood A K and Narayana C 2005 *Pramana* **64** 119
[22] Balbashov A M, Karabashev S G, Mukovskiy Ya M and Zverkov S A 1996 *J. Cryst. Growth* **167** 365
[23] Abrashev M V, Litvinchuk A P, Iliev M N, Meng R L, Popov V N, Ivanov V G, Chakalov R A and Thomsen C 1999 *Phys. Rev.* B **59** 4146
[24] Jandl S, Barilo S N, Shiryaev S V, Mukhin A A, Ivanov V Yu and Balbashov A M 2003 *J. Magn. Magn. Mater.* **264** 36
[25] Granado E, Garcia A, Sanjurjo J A, Rettori C, Torriani I, Prado F, Sanchez R D, Canairo A and Oseroff S B 1999 *Phys. Rev.* B **60** 11879
[26] Jandl S, Mukhin A A, Ivanov V Yu and Balbashov A M 2005 submitted
[27] Iliev M N and Abrashev M V 2001 *J. Raman Spectrosc.* **32** 805
[28] Podobedov V B, Weber A, Romero D B, Rice J P and Drew H D 1998 *Solid State Commun.* **105** 589
[29] Yamamoto K, Kimura T, Ishikawa T, Katsufuji T and Tokura Y 2000 *Phys. Rev.* B **61** 14706